

Joint Occurrence of Heatwaves and Ozone Pollution and Increased Health Risks in Beijing, China: Role of Synoptic Weather Pattern and Urbanization

Lian Zong¹, Yuanjian Yang^{1,*}, Haiyun Xia^{1,*}, Meng Gao², Zhaobin Sun³, Zuofang Zheng³, Xianxiang Li⁴, Guicai Ning⁵, Yubin Li¹, and Simone Lolli⁶

¹Collaborative Innovation Centre on Forecast and Evaluation of Meteorological Disasters, Key Laboratory for Aerosol-Cloud-Precipitation of China Meteorological Administration, School of Atmospheric Physics, Nanjing University of Information Science & Technology, Nanjing, China.

²Department of Geography, Hong Kong Baptist University, Hong Kong, China.

³Institute of Urban Meteorology, China Meteorological Administration, Beijing, China.

⁴School of Atmospheric Sciences, Sun Yat-Sen University, Guangzhou, China.

⁵Department of Land Surveying and Geo-Informatics, The Hong Kong Polytechnic University, Hong Kong, China.

⁶CNR-IMAA, Contrada S. Loja, 85050 Tito Scalo (PZ), Italy

Correspondence to: Prof. Yuanjian Yang (yyj1985@nuist.edu.cn) and Prof. Haiyun Xia (hsia@ustc.edu.cn)

Abstract. Heatwaves (HWs) paired with higher ozone (O₃) concentration at surface level pose a serious threat to human health. Their combined modulation of synoptic patterns and urbanization remains unclear. By using five years of summertime temperature and O₃ concentrations observation in Beijing, this study explored potential drivers of compound HWs and O₃ pollution events and their public health effects. Three-Three unfavourable synoptic weather patterns were identified to dominate the compound HWs and O₃ pollution events. These weather patterns contributing to enhance those conditions are characterized by sinking air motion, low boundary layer height, and hot temperatures. Under the synergistic of HWs and O₃ pollution, the mortality risk from all non-accidental causes increased by approximately 12.31% (95% confidence interval: 4.66%, 20.81%). Urbanization caused higher risks for HWs and O₃ at urban areas than rural stations. Under the synergistic stress of HWs and O₃ pollution, the public mortality risk increased by approximately 12.59% (95% confidence interval: 4.66%, 21.42%). Relative to rural areas, urbanization caused higher risks for HWs, but lower risks for O₃ over urban areas. Particularly, due to O₃ depletion caused by NO titration at traffic and urban stations, the health risks related to O₃ pollution in different regions are characterized as follows: suburban stations > urban stations > rural stations > traffic stations. In general, unfavourable synoptic patterns and urbanization enhanced the compound health risk of these compound events in Beijing by 45.46% and 33.09%, respectively. Our findings provide robust evidence and implications for forecasting compound heatwaves and O₃ pollution event and its health risks in Beijing or in other urban areas all over the world having high concentrations of O₃ and high-density populations.

Key words: Heatwaves, ozone pollution, compound health risks, synoptic weather pattern, urbanization

1 Introduction

Climate warming and rapid urbanization have led to an increase in the frequency and duration of extreme high-temperature episodes (Lehner et al., 2018; Meehl & Tebaldi, 2004; Wang et al., 2021b; Yang et al., 2017; Li, 2020). Such prolonged extreme high-temperature exposure can induce an increase in the morbidity and mortality due to cardiovascular and respiratory diseases, posing a serious threat to human health (Patz et al., 2005; Xu et al., 2016). Therefore, to the point that the extreme high-temperature events they are recognized as one of the most serious types of meteorological disaster worldwide. Prolonged extreme high-temperature exposure can induce an increase in the morbidity and mortality due to cardiovascular and respiratory diseases, posing a serious threat to human health (Patz et al., 2005; Xu et al., 2016). However, high temperatures during summer heatwaves are paired with serious O₃ pollution frequently, for instance, significantly increased O₃ concentrations have been observed in the UK and France during the August 2013 heatwave event (Lee et al., 2006; Vautard et al., 2005; Vautard et al., 2007). High concentrations of O₃ exposure would stimulate the human respiratory system, damage lung cells, and aggravate other chronic lung diseases (WHO, 2021), which poses a great threat to human health. Consequently, residents may suffer from dual health risks caused by both high temperatures and O₃ exposures in summer. Although extreme hot events have received extensive attention from academia and society, the research on health risks aroused by O₃ pollution associated with high temperature has been neglected. As a result, it might be greatly underestimated that the health risks to the human body enduringly exposed to the outdoors during hot days.

As a continuous extreme case of high temperature weather in summer, heat waves (HWs) have previously been shown by numerous epidemiological studies to cause significantly higher overall deaths than non-heatwave (NHW) periods (Conti et al., 2005; Fouillet et al., 2006). Subsequently, many scholars launched investigations on the relationship between high temperature exposure and mortality (Abbas and Tewtel-Salem, 2005; Huang et al., 2015; Zhang et al., 2017), and they found that when the temperature was higher than a certain threshold temperature, the mortality rate increased with the increase of temperature. Most studies suggested that there were a U-, V-, W-, or J-shaped non-linear change relationship between daily mortality and daily temperature (Goggins et al., 2012; Huang et al., 2015; Y. Zhang et al., 2017). Similar studies on O₃ concentration and mortality have also been progressing (Atkinson et al., 2012; Gu et al., 2018; Pope et al., 2016). Particularly, Accumulating some epidemiological evidences showed that the coefficient of the O₃ concentration–response relationship for mortality in summer was higher with respect to other seasons (Atkinson et al., 2012; Pattenden et al., 2010; Pope et al., 2016; Zhong et al., 2019), suggesting that the health effects and mortality related to O₃ pollution were exacerbated by hot temperatures. Therefore, the significant increase in O₃ concentrations during summertime is also greatly responsible for the increase in excess mortality.

that is, high temperatures and O₃ have exhibit a joint impact on public health (Hertig et al., 2020; Katsouyanni et al., 1993; Lelieveld et al., 2014; Pattenden et al., 2010). Numerous previous studies have been devoted to the individual impacts of a single extreme high-temperature or air pollution event on human health (Ma et al., 2015; Ning et al., 2020; Wang et al., 2020; Wong et al., 2013; Xu et al., 2016). However, with the co-occurrence of extreme HW and O₃ pollution events in summer

65 becoming more frequent, it is imperative to reveal the underlying mechanisms of extreme HW–O₃ compound events and to improve the level of risk assessment related to extreme events in urban areas (Sartor et al. 1995; Hertig et al., 2020).

Together with the rapid development of economic globalization and urbanization, human activities and the changes in the urban underlying surface have ~~enhanced~~ induced frequent occurrences of both extreme high surface urban hyperthermia-air temperature and frequent air pollution issues (Chew, et al., 2021; Li et al., 2016; Luo & Lau, 2018, 2019; Meehl et al., 2007; Rastogi, 2020; Wang et al., 2007; Yang et al., 2020; Zheng et al., 2020). Particularly, Heat waves (HWs) paired with the urban heat island (UHI) effect exposes urban residents to more sustained extreme high temperatures (Chew et al., 2021; Jiang et al., 2019; Tan et al., 2010; Wang et al., 2017; Zong et al., 2021b). Meanwhile, rapid urbanization induced many more also emissions of hydrocarbons and nitrogen oxides into the atmosphere from traffic vehicle and industries, the rising concentrations of these precursors coupled with high temperature and intense solar radiation during HWs accelerate photochemical reaction rate and generate more O₃ (Sillman, 1999; Yim et al., 2019; Zanis et al., 2000). As a result, urban residents ~~are may face more vulnerable to health risks posed by severe stresses from both heat and O₃ stress~~ pollutions. However, note that the improvement of economic level, medical infrastructure and air-conditioning utilization associated with urbanization can alleviate the health burden of the human body in the face of high temperature and O₃ exposure to a certain extent (Bai et al., 2016; Kovach et al., 2015; Li et al., 2017). Therefore, it can be concluded that there still are some uncertainties in affecting the excess mortality of high temperature and O₃ pollution. To sum up, clarifying the formation mechanism of HW– O₃ compound events and quantifying their health risks to urban residents are important scientific issues that warrant further investigation.

Beijing, the capital of China, is the second largest city in the country, with a permanent population of 21.89 million, ~~making~~ It is not only one of the fastest developing metropolises in China in recent decades, but also a typical heat island city. Rapid urbanization and urban expansion have induced changes in land use types, which in turn have changed the energy budget within the city boundary layer (Dou et al., 2015; Li et al., 2015; Wang et al., 2007; Yu et al., 2013; Zheng et al., 2018; Zinzi et al., 2020). Urban areas usually experience warmer temperatures compared with rural areas (Oke and Maxwell, 1975; Rizwan et al., 2008; Roth, 2007; Stewart and Oke, 2012), and this strong UHI effect can be observed in Beijing all year around (Ren et al., 2007; Wang et al., 2017; Yang et al., 2013). Taking Beijing as a typical example. Therefore, the present ~~is~~ study focuses on the health risks of extreme HW–O₃ compound events that occurred in Beijing during summertime of 2014–2019, was ~~carried out to~~ and comprehensively investigates the roles of synoptic weather patterns and urbanization in these joint ~~compound~~ events based on surface observation and reanalysis data. Then, the contributions of weather types and urbanization to the excess mortality brought about ~~induced~~ by combined heat and O₃ stress were quantified according to the established health assessment model of Liu et al. (2021) and Yin et al. (2017). The findings are expected to provide a scientific reference for the monitoring and forecasting of summertime HW–O₃ compound events and their health risks in Beijing from the perspective of synoptic patterns and urbanization in high-density mega cities.

~~The strong solar radiation and high temperatures in summer have accelerated the photochemical reaction, which is a proxy to the production and accumulation of O₃ (Herring et al., 2019; Shu et al., 2016; Zanis et al., 2000, 2011). In particular, O₃ became the main pollutant in summer (Fan et al., 2020; Gao et al., 2020b; Li et al., 2019; Wang et al., 2019; Saikawa et al., 2017), and thus residents may suffer from dual health risks brought about by high temperatures and O₃ exposure in summer.~~

域代码已更改

域代码已更改

Accumulating epidemiological evidence shows that the coefficient of the O₃ concentration–response relationship for mortality in summer is higher (Atkinson et al., 2012; Pattenden et al., 2010; Pope et al., 2016; Zhong et al., 2019), suggesting that the health effects and mortality related to O₃ pollution are exacerbated by hot temperatures. Therefore, the significant increase in O₃ concentrations during summertime is also greatly responsible for the increase in excess mortality; high temperatures and O₃ have a joint impact on public health (Hertig et al., 2020; Katsouyanni et al., 1993; Lelieveld et al., 2014; Pattenden et al., 2010). Numerous studies have been devoted to the individual impacts of a single extreme high temperature or air pollution event on human health (Ma et al., 2015; Ning et al., 2020; Wang et al., 2020; Wong et al., 2013; Xu et al., 2016). However, with the co-occurrence of extreme HW and O₃ pollution events in summer becoming more frequent, it is imperative to reveal the underlying mechanisms of extreme HW–O₃ compound events and improve the level of risk assessment related to extreme events in urban areas (Sartor et al., 1995; Hertig et al., 2020).

Beijing, the capital of China, is the second largest city in the country, with a permanent population of 21.89 million, making it one of the fastest developing metropolises in recent decades. Rapid urbanization and urban expansion have induced changes in land-use types, which in turn have changed the energy budget within the city boundary layer (Dou et al., 2015; Li et al., 2015; Wang et al., 2007; Yu et al., 2013; Zheng et al., 2018; Zinzi et al., 2020). Urban areas usually experience warmer temperatures compared with rural areas (Oke and Maxwell, 1975; Rizwan et al., 2008; Roth, 2007; Stewart and Oke, 2012), and this strong UHI effect can be observed in Beijing all year around (Ren et al., 2007; Wang et al., 2017; Yang et al., 2013). As a result, urban residents are more vulnerable to health risks posed by heat stress. On the other hand, the increased O₃ concentration induced by urbanization was found to translate to a 39.6% increase in premature mortality (Yim et al., 2019). Importantly, whilst urban greening might alleviate the UHI effect (Doick et al., 2014; Zhou et al., 2019), the additional biogenic volatile organic compounds (VOCs) emitted from vegetation under high temperature stress can favour O₃ production (Ma et al., 2019; Wang et al., 2021a; Werner et al., 2020). For example, Ma et al. (2019) found that the landscape in Beijing yields an extra 4.47 ppbv of MDA8-O₃ (the maximum daily 8-h average concentration of O₃) due to the increase in urban isoprene emissions associated with HWs, and the isoprene emitted from forests in rural areas should also not be underestimated. But what roles do synoptic weather patterns and urbanization play in the formation of complex HW–O₃ compound events in Beijing with its high population density? What are the public health effects caused by these compound events? These important scientific issues warrant further investigation.

Therefore, the present study on extreme HW–O₃ compound events that occurred in Beijing during summertime of 2014–2019 was carried out to comprehensively investigate the roles of synoptic weather patterns and urbanization in these joint events based on surface observation and reanalysis data. Then, the contributions of weather types and urbanization to the excess mortality brought about by combined heat and O₃ stress were quantified according to the established health assessment model

of Liu et al. (2021) and Yin et al. (2017). The findings are expected to provide a scientific reference for the monitoring and forecasting of summertime HW-O₃ compound events and their health risks in Beijing from the perspective of synoptic patterns and urbanization.

2 Data and Methods

135 2.1 Data

Ground-level O₃ observation data during summertime (June–August) of 2014–2019 were retrieved from Beijing Municipal Ecological and Environmental Monitoring Center. After quality control, and excluding stations with a missing-values rate for the O₃ concentration of more than 10%, ultimately comprising 31 air quality stations (AQSS; including 11 for urban stations, 11 for rural-suburban stations, three for traffic stations (road monitoring stations for traffic air quality), and six for other rural stations) are ultimately used in this study, with a missing-values rate for the O₃ concentration of less than 10%.

140

In order to better assess the relationship between O₃ pollution and the meteorological variables, we selected 29 automatic weather stations (AWSs) closest to the environmental monitoring stations from the high-density AWS network (Figure 1; Table 1). For specific geographic location information, see Figure 1 and Table 1. Hourly 2-m air temperature, relative humidity (RH), the daily maximum temperature (T_{max}), and 10-m wind speed (WS) of these 29 AWSs were obtained from the National Meteorological Information Center of the China Meteorological Administration, and then heat index (HI) was retrieved as shown in Rothfus (1990) as Eq. (1):

145

$$HI = -42.379 + 2.04901523 \times T + 10.14333127 \times RH - 0.22475541 \times T \times RH - 0.00683783 \times T^2 - 0.05481717 \times RH^2 + 0.00122874 \times T^2 \times RH + 0.00085282 \times T \times RH^2 - 0.00000199 \times T^2 \times RH^2, \quad (1)$$

Where T indicates the temperature (unit: °F), and RH (unit: %) indicates relative humidity.

150

In addition, we also used the hourly geopotential height (GH), boundary layer height (BLH), wind vector, vertical velocity and temperature fields to further analyze the weather type and local boundary layer characteristics under the joint occurrence of HW and O₃ pollution (Fifth major global reanalysis produced by the European Centre for Medium-Range Weather Forecasts, with spatiotemporal resolution of 0.25°).

2.2 Methods

155 2.2.1 Compound HW and O₃ pollution events

An HW event is usually characterized by the daily maximum temperature reaching or exceeding a certain threshold (it can be a relative value or an absolute threshold) for several consecutive days (Ngarambe et al., 2020). In this paper, we selected 33°C (which corresponds to the 90th percentile of T_{max} during 2014–2019 in Beijing) as threshold for T_{max} lasting for 3 days or more to determine an HW event; otherwise, it was a non-heat wave (NHW) event. Moreover, the occurrence of precipitation during the day inhibits the photochemical reaction of O₃ production (Yu et al., 2020; Zhang et al., 2015; Zhao and Wang, 2017), here

160

a daytime precipitation event (accumulated precipitation ≥ 2 mm during 0700–1900 LST) was excluded to avoid the impact of precipitation on compound HW and O₃ pollution events. O₃ pollution was identified as when the MDA8 O₃ concentration exceeded 160 $\mu\text{g m}^{-3}$, which is in accordance with the Ambient Air Quality Standards issued by the Ministry of Ecology and Environment of the People's Republic of China. Based on the above criteria, 84 days of co-occurring HW and O₃ pollution events during 2014–2019 were finally obtained.

2.2.2 Weather type classification

The T-mode principal component analysis (T-PCA) is an improved mathematical method to classify the circulation pattern, which has a low dependence on preset parameters, and has advanced temporal and spatial stability of classification (Richman, 1981; Huth et al., 2008). Consequently, T-PCA has been widely used in the studies of atmospheric circulation effects of extreme weather. According to previous studies (Han et al., 2020; Miao et al., 2019; Ning et al., 2019; Yang et al., 2018, 2021; Zhang and Villarini, 2019), (Zong et al., 2021; Miao et al., 2019; Ning et al., 2019; Yang et al., 2018, 2021; Zhang and Villarini, 2019). It decomposes the original data matrix into the product of the principle component matrix and the load matrix (two low-dimensional matrices), then rotates the first r ($r \leq n$) principal components with larger variance contributions obliquely, and finally obtains the synoptic patterns and classifications of each time according to the magnitude of the load (Huth et al., 2000). T-mode principal component analysis (T-PCA) Here, T-PCA was applied in COST733class to classify the 850-hPa GH field of the joint occurrence of HW and O₃ pollution events and the number of classifications was determined based on the explained cluster variance. [more specific details on T-PCA were introduced in our previous study (Zong, et al., 2021a)]. As for the categorical data, we mainly focused on the domain (110°–125°E, 32°–47°N), including Beijing, associated with these 84 days of compound events during summertime (June–August) 2014–2019.

2.2.2 Excess mortality

In epidemiology, the relative risk (RR) is usually used to evaluate the intensity of the association between exposure and disease, which refers to the ratio of the incidence of the exposed group to the incidence of the non-exposed group (Chen et al., 2018; Pope et al., 2016). The RR is calculated by Eq. (2):

$$RR_i = \exp^{\beta_i \Delta X_i}, \quad (2)$$

where i indicates the risk factor (high temperature or O₃ concentration), β_i is the coefficients of the exposure response function between the risk factor i and total mortality through nonlinear regression (Cao et al., 2021; Du et al., 2020; Gu et al., 2018), ΔX_i is the difference between the risk factor i and its reference health threshold. The excess risk (ER) is calculated by Eq. (3):

$$ER_i = (RR_i - 1) \times 100\%, \quad (3)$$

In the previous studies on the health risks of high temperature and O₃ in China, the sensitivity of human morbidity and mortality caused by high temperature and O₃ overexposure to different geographic regions is quite different (Huang et al., 2015; Ma et al., 2015; Wang et al., 2020; Yin et al., 2017). For instance, (Huang et al., 2015) revealed that for a 1°C increase above the minimum mortality temperature, the daily mortality increased by 1.04% [95% confidence interval (CI): 0.90 to 1.18], 1.25

(95% CI: 0.71 to 1.79), 1.19 (95% CI: 0.79 to 1.58), and 1.38 (95% CI: 0.54 to 2.23) in the nationwide, central China, eastern China, and south China, respectively. Here, we refer to the exposure response function for the high temperature as suggested by Liu et al. (2021), and O₃ concentration as suggested by Yin et al. (2017) in northern China. In detail, Liu et al. (2021) investigated the mortality caused by high temperature in 84 cities in China from 2013 to 2016, and found that for every 1°C increase in the daily T_{max} above 31.5°C, the largest RR of mortality caused by high temperature in northern China was 1.002 (95% confidence interval (CI): 1.001, 1.004). According to Eq. (2), we can deduce that β_{Tmax}=0.997% (95% CI: 0.996%, 0.999%), it is worth noting that when T_{max}=31.5°C, RR=1. For O₃ exposure, a 10-μg m⁻³ increase in MDA8 O₃ was related to an increase in the total daily mortality of 0.39% (95% CI: 0.04%, 0.75%) in northern China during the warm season (Yin et al., 2017), that is to say, β_{Ozone}=0.39% (95% CI: 0.04%, 0.75%). Since the two models have removed the mutual influence, the final joint ER is the sum of the ERs of both high temperature and O₃.

2.2.3 Urbanization and Synoptic contribution rates

To estimate the impact of urbanization and weather patterns on compound HW and O₃ pollution events, we further determined their contribution rates to the excess mortality of compound events. With reference to Ma & Yuan (2021) and Yang et al. (2017), the urbanization effect is calculated by Eq. (4):

$$\Delta ER_{i,urbanization} = ER_{i,urban} - ER_{i,rural}, \quad (4)$$

and contribution rate is calculated by Eq. (5):

$$CR_{i,urbanization} = \frac{\Delta ER_i}{ER_{i,urban}} \times 100\%, \quad (5)$$

Where *i* indicates risk factor (high temperature or ozone pollution), ER is excess mortality, and CR is contribution rate.

Similarly, we also defined synoptic effects as Eq. (6):

$$\Delta ER_{i,synoptic} = ER_{i,synoptic} - ER_{i,average}, \quad (6)$$

and the contribution rate as Eq. (7):

$$CR_{i,synoptic} = \frac{\Delta ER_i}{ER_{i,synoptic}} \times 100\%, \quad (7)$$

Where *i*, ER, and CR are same as Eq. (6).

3 Results

3.1 Compound HW–O₃ pollution events and associated public health in Beijing

Figure 2 shows the time series of the HW-days, NHW-days, O₃ pollution, and precipitation days, and the interannual and intraseasonal variations of HW and O₃ pollution days. For interannual variation, the total days of O₃ pollution in summer was relative stable, while the total days of HW increased slightly. For intraseasonal variation, O₃ pollution was the most serious in June, while the most frequently HW events in July. Obviously, showing that higher O₃ pollution levels (>160 μg m⁻³) were

always accompanied by most HW periods (approximately 79.2% of HW days) in Beijing, (Figures 2a and 3b), in Beijing, were always paired above threshold O₃ pollution levels, which were mainly in the middle of summer. Daytime precipitation obviously inhibits the photochemical reaction with consequent fewer O₃ pollution episodes occurred during daytime precipitation (the average 24 h O₃ concentration was reduced by 17.14 μg m⁻³ on precipitation days compared with NHW days). In addition, Note note that there was an increase in the maximum duration of HW events and the number of HW-O₃ paired days during summertime of 2014–2019 (Figure 3), by especially in 2019, when the most durable HW event lasted for 10 days), resulting in people suffering from more extreme enduring dual heat and O₃ stresses to residents. As shown in Figure 4, relative to NHW days, MDA8 O₃ aggravated increased significantly on HW days, exceeding 160 μg m⁻³ across all stations, with an average of 189.35 μg m⁻³. Nevertheless, also during NHW days, some MDA8 O₃ stations (mainly urban or vegetation covered stations) exceeded the pollution threshold. Both surface O₃ concentration and MDA8 O₃ concentration in Beijing showed significant differences ($P < 0.001$) through analysis of variance among three conditions (Table S1). Therefore in general, it can be concluded that the difference in O₃ concentration was mainly due to meteorological conditions and the precursors emission paired with photochemical reactions in the boundary layer without considering O₃ emission precursors. We further investigated the diurnal variation for surface air temperature (T), RH, HI, BLH and WS under HW, NHW and precipitation periods (Figure 5), and these five variables also showed significant differences (passed the Kruskal-Wallis test of 0.001, more details see Table S2) in the three periods. For HW days, HI was aggravated raised more by increased air temperature, and although the RH was relative lower, people still suffered from higher apparent temperature than actual air temperature. During Under HW conditions, solar radiation reaching the ground heats the atmosphere increasing the near-surface temperature. Warmer air convection promotes atmospheric instability, with increased WS and higher BLH. It is clear that the meteorological variables during at daytime were significantly different during HW periods were significantly different than under other conditions with respect to NHW periods, and similarly, hourly O₃ concentrations also showed significantly difference under different meteorological conditions, and reached the peaks in the afternoon on HW days under these conditions reached the peaks (Figure 5f). Note that the contribution of local and regional emissions (transport of pollution between urban and rural areas) to air quality at a city scale should be focused (Thunis et al., 2021), which can also induce urban-rural differences. We assumed that the intraseasonal differences in precursor emissions can be ignored, and further compared the diurnal variation differences in NO₂, CO and O₃ among different stations (Figure 6). CO and NO₂ levels were higher at traffic stations than urban and suburban stations due to enhanced emission from vehicles, and the lowest CO and NO₂ levels appeared at rural stations. Generally speaking, high precursor levels are supposed to correspond to high resultants levels, but the lowest O₃ levels were found at traffic stations, followed by rural stations, then urban and suburban stations. Since automobile exhaust in the traffic and urban stations also caused heavily NO emission (Colville et al., 2001), ambient O₃ can be titrated by NO via the reaction $\text{NO} + \text{O}_3 \rightarrow \text{NO}_2 + \text{O}_2$ (Gao et al., 2020; Murphy et al., 2007; Sillman, 1999), this process in turn led to higher NO₂ levels and the loss of O₃ in traffic and urban areas. As for rural stations, low pollutant emissions may be the primary reason for the lower O₃ levels. Note that although the CO and NO₂ emissions were significantly higher at urban stations than those of suburban stations, there was less difference in O₃ concentrations between these two-type stations, which may be due

to O₃ consumption induced by titration at urban stations, or more biogenic VOCs at suburban stations. This is because that the difference in O₃ concentrations between the rural and the suburban stations were the largest in the afternoon, while the difference in CO and NO₂ levels were the smallest indicating that anthropogenic emissions have less impact in suburban areas, coupled with more than half of suburban stations are covered by vegetations leading to more bio-VOC emissions. Therefore, it can be concluded that the difference in O₃ concentration was mainly due to meteorological conditions paired with photochemical reactions in the boundary layer without considering O₃ emission precursors.

Moreover, the high temperatures on HW days not only brought induce a higher public risk related to high-temperature exposure, but also an increase in mortality related to O₃ exposure. During HW periods, high temperatures and strong solar radiation accelerate the rate of the photochemical reaction that produces O₃ (Pu et al., 2017; Sun et al., 2017), favouring the production and accumulation of O₃, thereby aggravating health risks. Regardless of the For -all-type of stations, the health risks related to the both O₃ and high-temperature-stressful conditions suffered by the population during HW days has greatly increased during HW days. Specifically, for all stations, HWs have increased the ER caused by high temperatures and O₃ by 3.867% (90% CI: 3.863%, 3.875%) and 7.9% (90%CI: 0.78%, 15.78%), respectively (Table 32). The high temperature risks were mainly manifested as followings: urban stations > traffic stations > suburban stations > rural stations, but the health risks aroused by O₃ exposure in different underlying surface stations were more difficult to quantifying due to the complexity of O₃ photochemical reactions. As mentioned above, interestingly, urbanization-enhanced NO or CO titration reduced more O₃ loss in urban areas, which was more pronounced over traffic stations. For suburban stations, the abundant biogenic VOC emitted by vegetation also contributed to O₃ generation, bio-VOC emissions enhanced more especially in hot days (Ma et al., 2019; Trainer et al., 1987; Wang et al., 2021a). As a result, O₃ exposure risks in Beijing were mainly characterized by suburban stations > urban stations > rural stations > traffic stations. Urbanization seems to have increased the ER induced by both high temperatures and O₃ exposure. In details, summertime HW, O₃ and compound ER increased by 1.67%, 0.20%, and 1.89%, respectively, compared to rural stations. Note that urbanization has alleviated O₃ pollution to a certain extent, and the health risk of O₃ at stations with developed transportation was even lower than that of rural stations, over urban stations by 39.88%, but caused a 2.44% reduction in the ER associated with O₃. On the one hand, high temperatures and strong solar radiation during HW periods accelerate the rate of the photochemical reaction that produces O₃ (Pu et al., 2017; Sun et al., 2017), which is conducive to the production and accumulation of O₃. On the other hand, they increase the VOC emission of plants and contributes to the production of O₃ (Ma et al., 2019; Trainer et al., 1987; Wang et al., 2021a). The majority of the isoprene emissions from forests in Beijing are mainly located in rural areas (Ma et al., 2019). Therefore, the O₃ concentrations over rural stations were higher than those over urban stations. In addition, the risk of O₃ exposure in the traffic stations was significantly lower than that of the urban and rural stations, and the risk of high temperature exposure was slightly lower than that of urban stations. This has also led to the overall paired high temperature and O₃ risk over traffic stations being lower than that over rural stations.

3.2 Role of synoptic weather pattern and urbanization

To further clarify the mechanism underlying the joint occurrence of HW-O₃ events in Beijing, three unfavourable synoptic weather patterns were identified as follows: (1) Type 1, characterized by the western Pacific subtropical high (WPSH) being located in the southeast of Beijing with prevailing southwesterly winds; (2) Type 2, controlled by a high-pressure system accompanied by weak southerly winds; and (3) Type 3, a low-vortex located over northeast Beijing with prevailing northwesterly winds (Figures 6a7a–6e7c, and detailed HW-O₃ date and type see Table S4). Additionally, vertical cross-sections of the potential temperature and wind vectors at 1400 LST under the three patterns are shown in Figures 6e7c–6f7f.

Under Type 1, low boundary layer paired with weak vertical motion favours pollutants' accumulation. Besides, the prevailing southwesterly wind may blow pollutants from the upwind direction to Beijing, and the northern mountains block the pollutants from continuing to be transported in the downward wind direction, causing the pollutants to gather in Beijing. For Type 2, a lower BLH and vertical convection together regulate the transportation and accumulation of O₃ in the boundary layer. Under Type 3, there is a valley–plain wind circulation in the boundary layer, and the strong downdraft over urban areas and the higher boundary layer cause the lowest MDA8 O₃ concentrations among the three weather types.

Overall, Type 1 tends to be associated with the highest excess mortality caused by O₃, and Type 3 is related with the highest excess mortality caused by HWs. For excess mortality induced by the HW-O₃ compound events, Type 1 (12.59%) > Type 3 (12.05%) > Type 2 (11.66%). Although there is little difference in the HW-O₃ compound ER under the three weather types, the mechanisms of the three types are quite different. Under the modulation of weather circulation and boundary layer meteorological elements, Type 1, Type 2 and Type 3 were associated with high O₃ and intermediate T_{max} exposure, intermediate O₃ and low T_{max} exposure, and low O₃ and high T_{max} exposure (Figure 78 and Table 3), respectively. Therefore, the synoptic weather pattern plays an important role in regulating the formation mechanism of HW-O₃ compound events, which also further leads to it having a significant impact on morbidities and deaths caused by HW-O₃ compound events.

To sum up, urbanization shows a positive regulation on health risks of O₃ and high-temperature under different synoptic weather patterns. Table 4 also shows that there was an opposite urbanization regulation effect between high temperature and O₃ and their health risks under Type 1. In particular, HWs extended the urban–rural air temperature difference (the UHI effect) in Beijing (Table 2), as which was also found in our previous study (Zong et al., 2021b). That is, the urbanization effect on health risk associated with heat exposure was amplified during hot days. But for O₃ pollution, urbanization and anthropogenic activities have significantly increased the emission of pollutants. On the one hand, it promotes photochemical reactions to generate O₃ during HW days. On the other hand, the titration of NO and CO in cities can deplete O₃. It was mentioned earlier that the O₃ pollution in rural areas is higher than that in urban areas during HW periods. For Under Type 1, the strong southerly airflow caused the horizontal transportation of O₃ and its precursors from the southwest (urban) to the northeast (suburban and rural), which is favourable for the accumulation of pollutants under the topography of Yanshan Mountains (to the north of Beijing). Therefore, urban-rural differences in O₃ concentration were narrowed, and the risk related to O₃ exposure in the suburban areas were the greatest under this weather pattern. Paired with the large number of forests in rural areas during the

HW that emitted additional VOCs (Ma et al., 2019), this further increased the difference in the O₃ concentration between urban and rural areas. Urbanization has a positive regulatory effect on the risk of heatwaves, but a negative one with respect to the risk of O₃. As for Type 2, Type 3 is mainly dominated by the northerly airflow at 850 hPa and the southerly wind at the lower level, the transport of local circulation has a weak adjustment to the urban-rural difference of O₃. However, the BLH difference between urban and rural areas (north-south difference) should be responsible for the decrease in urban-rural difference of health risk induced by O₃ concentration. For the stable weather and lower BLH under Type 2, the difference in O₃ concentration between urban and rural areas was the largest. and Type 3, there was a little difference in O₃ exposure risk between urban and rural areas, but urban residents were more likely to be exposed to higher-temperature environment under Type 3 compared to Type 2. Based on statistical analysis, Specifically, the contribution rates of urbanization to the excessive mortality caused by high temperatures and O₃ exposure were 27.7245.68% and -2.585.05%, respectively, while 80.21% and 13.9% the contribution rates of the caused by synoptic pattern, respectively were 85.54% and 24.00%. In summary, urbanization and the synoptic pattern respectively contributed 8.0818.95% and 4533.09% to the total HW-O₃ excess mortality (Table 54).

带格式的: 突出显示

4 Discussions

In addition to heatstroke, heat exhaustion, heat fainting and heat cramps and other diseases, high temperature during HW days can also lead to increased mortality of residents. Several studies have proposed that the mortality because of respiratory diseases, cardiovascular diseases and cardiopulmonary diseases induced by high temperature and O₃ exposure is particularly relevant (Chen et al., 2018; Du et al., 2020; Hu et al., 2019). Therefore, patients with pre-existing conditions as respiratory and cardiovascular diseases, should pay more attention and limit outdoor activity under heatwaves and O₃ polluted days. Furthermore, demographic, and socio-economic factors related to the level of urbanization, including age structure, education and healthcare services, occupational types, and air-conditioning use, also greatly affect the exposure response function of high temperature and O₃. For instance, females, elderly and people with a lower degree of instruction have suffered significantly higher health risks from overexposure of high temperature and O₃ than the average population (Huang et al., 2015; Yin et al., 2017; Zhang et al., 2017). However, this study mainly considers mortality by all-causes for all the population caused by high temperature and O₃ exposure. Health risks for high-risk groups such as the elderly, children, and patients with cardiovascular and respiratory diseases should be higher than our results. Consequently, especially during synoptic weather patterns that can cause paired HW and O₃ pollution events, the responsible departments should strengthen the risk management of extreme compound events such as HW and O₃ pollution, establish an early warning system, configure emergency plans, strengthen the health precautions of respiratory and cardiovascular diseases, as well as the elderly and other vulnerable groups, and protect public health.

To date, there is no exact consensus on urbanization effects on risk of paired high temperature and O₃ exposure. Previously, a common perception was that urban residents were more prone to risks of heat effect in the context of global warming and UHI effect (Clarke, 1972; Goggins et al., 2012; Heaviside et al., 2017). Indeed, air temperature is one of the main reasons dominate

the change in excess mortality caused by compound HW and O₃ events, In terms of the urban areas, the higher density of buildings, roads and population, greater heat capacity and anthropogenic heat, temperature of urban areas is significantly higher than that of rural areas (Roth, 2007; Stewart & Oke, 2012). The heatwaves increase the urban and rural areas temperature difference, as well as the maximum temperature difference, so urban residents may expose to a higher temperature environment. However, the urban-rural difference in O₃ concentration modulated by HW days is inconsistent with that in temperature. Since urban O₃ can be consumed by NO titration (Gao et al., 2020; Murphy et al., 2007; Sillman, 1999), urbanization alleviates the ozone exposure risk of residents to a certain extent. ~~Rural~~ But suburban forests emit additional VOCs that generate O₃ during hot days (Ma et al., 2019; Wang et al., 2021a; Werner et al., 2020), resulting in O₃ pollution slightly lower in urban than ~~rural~~ suburban areas(Gao et al., 2020). Based on the regional exposure response function model, urban areas suffer from higher mortality related to high temperature, while ~~rural~~ suburban areas experience higher public mortality associated with O₃ pollution. Overall, there is little difference in the risk of O₃ exposure from urbanization. It should be highlighted that also urbanization brought also some positive aspects. For example, a better economic level and medical conditions, can help to prevent more deaths to a certain extent; high air-conditioning utilization rate can also effectively reduce heat exposure; and the reduction in the proportion of highly exposed people engaged in agriculture, forestry and animal husbandry in urban areas also greatly reduces the risk of outdoor high-temperature and O₃ overexposure. As a result, rural residents are more vulnerable to face the dual high temperature and O₃ stress, and their exposure response function coefficients may also be higher than that of urban residents (Hu et al., 2019; Kovach et al., 2015; Li et al., 2017; Williams et al., 2013; Xing et al., 2020; Zhang et al., 2017). This also means that under co-occurring heatwaves and ozone-polluted weather patterns, vulnerable groups in the suburbs should be warned on the risks of outdoor activity and limiting their exposure to the pollutants.

Regarding with the paired HW–O₃ events, though we moved a step forward in exploring role of synoptic weather pattern and urbanization, there are still some limitations in our study. As mentioned earlier, in a specific area, the health risks faced by residents adjusted by different levels of urbanization may be quite different. Moreover, the high temperature and O₃ compound health risk model for special populations (e.g., patients with cardiovascular and respiratory diseases, the elderly, children, etc.) can also be further established and analyzed. Therefore, in the future research on compound climate and pollution health impacts it is necessary to consider a more refined discussion in a city based on the level of urbanization and among different population groups.

5 Conclusions

In this study, the complex mechanism of co-occurring HW–O₃ events in the boundary layer in Beijing was systematically investigated by combining meteorological observations, environmental monitoring observations, and reanalysis data, and the regulatory role on health risks induced by such compound events was explained from the perspective of the synoptic pattern and urbanization.

The Beijing area not only experienced a stronger UHI effect during the summertime high-temperature HWs, but was also often accompanied by more serious O₃ pollution. In the period under study, the max temperature T_{max} and MDA8 O₃ concentrations during HW days were ~4.21°C and ~37.98 µg m⁻³ higher than those on NHW days, respectively, excluding rainy daytime days. When people are exposed to the dual stress of high temperatures and O₃ pollution during on-HW-O₃ days, the increase in T_{max} and MDA8 O₃ concentrations is associated with an ~~12.31%~~ ~~(95% CI: 4.66%, 20.81%)~~ ~~11.78%~~ ~~(95% CI: 4.66%, 19.66%)~~ higher excess mortality from all non-accidental causes. Three unfavourable synoptic weather patterns that dominate such compound events and were identified as: (1) Type 1, a high-pressure system located in the southeast of Beijing and accompanied by southwesterly winds, under which the weak downdraft and relative stable boundary layer weaken the vertical mixing of O₃ and induce heavy O₃ pollution, consequently meaning that people consistently experience high health risks; (2) Type 2, in which Beijing is under the influence of a high-pressure system accompanied by weak southerly winds and sinking airflow in the boundary layer that favours O₃ transport together with its precursors. This translates into a lower excess mortality under Type 2 with respect to Type 1; and (3) Type 3, a low-pressure system located in the northeast of Beijing accompanied by northwesterly winds. Under this type, people endure stronger heat stress owing to higher temperatures and lower RH, but the higher BLH and large atmospheric environment capacity alleviate O₃ exposure to a certain extent, which results in a decrease in O₃ concentration and ER compared with the other two patterns. Overall, the unfavourable weather types contributed ~~45.76~~ ~~33.09%~~ to the excess mortality attributed to the HW-O₃ compound events.

In addition, urbanization has also exacerbated the combined health risks of high temperature and O₃ pollution, which contributed ~~8.08~~ ~~18.95%~~. During the co-occurring HW-O₃ days, urbanization greatly affected the increase in high temperatures and related excess mortality risks in urban areas, which were significantly higher than those in rural areas. ~~On the contrary~~ However, O₃ pollution and its health risks in urban areas were ~~slightly lower~~ ~~higher~~ than those in rural areas, and ~~the contribution of urbanization effects was attenuated due to the reaction of O₃ and NO_x~~ ~~negative~~. ~~Note that O₃ pollution and its health risks in suburban areas were quite prominent due to less O₃ depletion and more bio-VOCs emissions. This is because those urban pollutants (O₃ and its precursors) were diffused and transported to the rural areas via local urban island circulation, which greatly increased the O₃ pollution and resultant excess mortality risk in rural areas, and reduced the O₃ concentration and related health risks in urban areas.~~

In summary, our findings help to better understand the formation mechanism of HW-O₃ compound events in Beijing, with robust supporting evidence from the perspective of synoptic patterns and urbanization. Our results also suggest that forecasting of identified synoptic patterns could help to avoid exposure of compound HW-O₃ events. However, the urbanization effect has ~~an opposite~~ ~~different~~ regulatory effect on HWs and O₃, meaning that high temperatures and O₃ exposure is deserving of the establishment of a more refined health model that takes into account the differences between urban and rural areas.

Data availability

415 The datasets that are analyzed and used to support the findings of this study are available in the public domains: The ground-level O₃ observation data can be obtained from Beijing Municipal Ecological and Environmental Monitoring Center (<http://www.bjmemc.com.cn/>, last access on November 20, 2021). The hourly meteorological data can be obtained from the National Meteorological Information Center of the China Meteorological Administration (<http://data.cma.cn/>, last access on November 20, 2021). The ERA5 reanalysis data set is available at the European Centre for Medium-Range Weather Forecasts
420 (<https://cds.climate.copernicus.eu/cdsapp#!/home>, last access on November 20, 2021).

Competing interests

The authors declare that they have no conflict of interests.

Author contributions

L. Zong: Methodology, Data Curation, Formal Analysis, Writing- Original draft preparation, Results Discussion, Writing-
425 Reviewing and Editing; Y. Yang, H. Xia: Conceptualization, Methodology, Formal Analysis, Results Discussion, Writing-
Reviewing and Editing; Z. Sun, Z. Zheng, X. Li, G. Ning, Y. Li, S. Lolli: Results Discussion, Comments, Writing- Reviewing
and Editing.

Acknowledgments

This research was supported by the National Natural Science Foundation of China (42175098).

430 **References**

- Abbas, E.-Z. and Tewtel-Salem, M.: On the association between high temperature and mortality in warm climates, *Sci. Total Environ.*, 343(1–3), 273–275, doi:10.1016/j.scitotenv.2004.12.024, 2005.
- Atkinson, R. W., Yu, D., Armstrong, B. G., Pattenden, S., Wilkinson, P., Doherty, R. M., Heal, M. R. and Anderson, H. R.: Results from Five Urban and Five Rural U . K . Populations, *Environ. Health Perspect.*, 120(10), 1411–1417, 2012.
- 435 Bai, L., Woodward, A., Cirendunzhu and Liu, Q.: County-level heat vulnerability of urban and rural residents in Tibet, China, *Environ. Heal.*, 15, doi:10.1186/s12940-015-0081-0, 2016.
- Cao, R., Wang, Y., Huang, J., Zeng, Q., Pan, X., Li, G. and He, T.: The construction of the air quality health index (AQHI) and a validity comparison based on three different methods, *Environ. Res.*, 197(March), 110987, doi:10.1016/j.envres.2021.110987, 2021.

- 440 Chen, R., Yin, P., Wang, L., Liu, C., Niu, Y., Wang, W., Jiang, Y., Liu, Y., Liu, J., Qi, J., You, J., Kan, H. and Zhou, M.: Association between ambient temperature and mortality risk and burden: Time series study in 272 main Chinese cities, *BMJ*, 363(k4306), doi:10.1136/bmj.k4306, 2018.
- Chew, L. W., Liu, X., Li, X. X. and Norford, L. K.: Interaction between heat wave and urban heat island: A case study in a tropical coastal city, Singapore, *Atmos. Res.*, 247(2020), 105134, doi:10.1016/j.atmosres.2020.105134, 2021.
- 445 Clarke, J. F.: Some effects of the urban structure on heat mortality, *Environ. Res.*, 5(1), 93–104, doi:10.1016/0013-9351(72)90023-0, 1972.
- Colville, R. N., Hutchinson, E. J., Mindell, J. S. and Warren, R. F.: The transport sector as a source of air pollution, *Atmos. Environ.*, 35(9), 1537–1565, doi:10.1016/S1352-2310(00)00551-3, 2001.
- Du, X., Chen, R., Meng, X., Liu, C., Niu, Y., Wang, W., Li, S., Kan, H. and Zhou, M.: The establishment of National Air Quality Health Index in China, *Environ. Int.*, 138(2019), 105594, doi:10.1016/j.envint.2020.105594, 2020.
- 450 Gao, L., Yue, X., Meng, X., Du, L., Lei, Y., Tian, C. and Qiu, L.: Comparison of Ozone and PM_{2.5} Concentrations over Urban, Suburban, and Background Sites in China, *Adv. Atmos. Sci.*, 37(12), 1297–1309, doi:10.1007/s00376-020-0054-2, 2020.
- Goggins, W. B., Chan, E. Y. Y., Ng, E., Ren, C. and Chen, L.: Effect modification of the association between short-term meteorological factors and mortality by urban heat islands in Hong Kong, *PLoS One*, 7(6), e38511, doi:10.1371/journal.pone.0038551, 2012.
- 455 Gu, Y., Wong, T. W., Law, S., Dong, G., Ho, K. F., Yang, Y. and Yim, S. H. L.: Impacts of sectoral emissions in China and the implications: Air quality, public health, crop production, and economic costs, *Environ. Res. Lett.*, 13, doi:10.1088/1748-9326/aad138, 2018.
- 460 Han, H., Liu, J., Shu, L., Wang, T. and Yuan, H.: Local and synoptic meteorological influences on daily variability in summertime surface ozone in eastern China, *Atmos. Chem. Phys.*, 20(1), 203–222, doi:10.5194/acp-20-203-2020, 2020.
- Heaviside, C., Macintyre, H. and Vardoulakis, S.: The Urban Heat Island: Implications for Health in a Changing Environment, *Curr. Environ. Heal. reports*, 4(3), 296–305, doi:10.1007/s40572-017-0150-3, 2017.
- Hertig, E., Russo, A. and Trigo, R. M.: Heat and ozone pollution waves in central and south Europe—characteristics, weather types, and association with mortality, *Atmosphere (Basel)*, 11(12), 1–18, doi:10.3390/atmos11121271, 2020.
- 465 Hu, K., Guo, Y., Hochrainer-Stigler, S., Liu, W., See, L., Yang, X., Zhong, J., Fei, F., Chen, F., Zhang, Y., Zhao, Q., Chen, G., Chen, Q., Zhang, Y., Ye, T., Ma, L., Li, S. and Qi, J.: Evidence for urban–rural disparity in temperature–mortality relationships in Zhejiang Province, China, *Environ. Health Perspect.*, 127(3), 1–11, doi:10.1289/EHP3556, 2019.
- Huang, Z., Lin, H., Liu, Y., Zhou, M., Liu, T., Xiao, J., Zeng, W., Li, X., Zhang, Y., Ebi, K. L., Tong, S., Ma, W. and Wang, L.: Individual-level and community-level effect modifiers of the temperature–mortality relationship in 66 Chinese communities, *BMJ Open*, 5(9), doi:10.1136/bmjopen-2015-009172, 2015.
- 470 Jiang, S., Lee, X., Wang, J. and Wang, K.: Amplified Urban Heat Islands during Heat Wave Periods, *J. Geophys. Res. Atmos.*, 124(14), 7797–7812, doi:10.1029/2018JD030230, 2019.

- Katsouyanni, K., Pantazopoulou, A., Touloumi, G., Tselepidaki, I. and Moustris, K.: Archives of Environmental Health : An
 475 International Evidence for Interaction between Air Pollution and High Temperature in the Causation of Excess Mortality
 Evidence for Interaction between Air Pollution and High Temperature in the Causation of Excess Mor, Arch. Environ. Heal.
 An Int. J., 48(4), 235–242, doi:10.1080/00039896.1993.9940365, 1993.
- Kovach, M. M., Konrad, C. E. and Fuhrmann, C. M.: Area-level risk factors for heat-related illness in rural and urban
 locations across North Carolina, USA, Appl. Geogr., 60, 175–183, doi:10.1016/j.apgeog.2015.03.012, 2015.
- 480 Lehner, F., Deser, C. and Sanderson, B. M.: Future risk of record-breaking summer temperatures and its mitigation, Clim.
 Change, 146(3–4), 363–375, doi:10.1007/s10584-016-1616-2, 2018.
- Lelieveld, J., Hadjinicolaou, P., Kostopoulou, E., Giannakopoulos, C., Pozzer, A., Tanarhte, M. and Tyrlis, E.: Model
 projected heat extremes and air pollution in the eastern Mediterranean and Middle East in the twenty-first century, Reg.
 Environ. Chang., 14(5), 1937–1949, doi:10.1007/s10113-013-0444-4, 2014.
- 485 Li, Y., Odame, E. A., Silver, K. and Zheng, S.: Comparing Urban and Rural Vulnerability to Heat-Related Mortality: A
 Systematic Review and Meta-analysis, J. Glob. Epidemiol. Environ. Heal., 1(1), 9–15, doi:10.29199/geeh.101016, 2017.
- Liu, J., Ai, S., Qi, J., Wang, L., Zhou, M., Wang, C., Yin, P. and Lin, H.: Defining region-specific heatwave in China based
 on a novel concept of “avoidable mortality for each temperature unit decrease,” Adv. Clim. Chang. Res., 12(5), 611–618,
 doi:10.1016/j.accre.2021.08.002, 2021.
- 490 Liu, N., Zhou, S., Liu, C. and Guo, J.: Synoptic circulation pattern and boundary layer structure associated with PM2.5
 during wintertime haze pollution episodes in Shanghai, Atmos. Res., 228(46), 186–195, doi:10.1016/j.atmosres.2019.06.001,
 2019.
- Luo, M. and Lau, N. C.: Increasing Heat Stress in Urban Areas of Eastern China: Acceleration by Urbanization, Geophys.
 Res. Lett., 45(23), 13,060–13,069, doi:10.1029/2018GL080306, 2018.
- 495 Luo, M. and Lau, N. C.: Urban Expansion and Drying Climate in an Urban Agglomeration of East China, Geophys. Res.
 Lett., 46(12), 6868–6877, doi:10.1029/2019GL082736, 2019.
- Ma, M., Gao, Y., Wang, Y., Zhang, S., Ruby Leung, L., Liu, C., Wang, S., Zhao, B., Chang, X., Su, H., Zhang, T., Sheng,
 L., Yao, X. and Gao, H.: Substantial ozone enhancement over the North China Plain from increased biogenic emissions due
 to heat waves and land cover in summer 2017, Atmos. Chem. Phys., 19(19), 12195–12207, doi:10.5194/acp-19-12195-2019,
 500 2019.
- Ma, W., Zeng, W., Zhou, M., Wang, L., Rutherford, S., Lin, H., Liu, T., Zhang, Y., Xiao, J., Zhang, Y., Wang, X., Gu, X.
 and Chu, C.: The short-term effect of heat waves on mortality and its modifiers in China: An analysis from 66 communities,
 Environ. Int., 75, 103–109, doi:10.1016/j.envint.2014.11.004, 2015.
- Meehl, G. A. and Tebaldi, C.: More Intense , More Frequent , and Longer Lasting Heat Waves in the 21st Century, Science
 505 (80-.), 305(5686), 994–997, doi:10.1126/science.1098704, 2004.
- Meehl, G. A., Arblaster, J. M. and Tebaldi, C.: Contributions of natural and anthropogenic forcing to changes in temperature
 extremes over the United States, Geophys. Res. Lett., 34(August), 1–5, doi:10.1029/2007GL030948, 2007.

- Miao, Y., Liu, S. and Huang, S.: Synoptic pattern and planetary boundary layer structure associated with aerosol pollution during winter in Beijing, China, *Sci. Total Environ.*, 682, 464–474, doi:10.1016/j.scitotenv.2019.05.199, 2019.
- 510 Murphy, J. G., Day, D. A., Cleary, P. A., Wooldridge, P. J., Millet, D. B., Goldstein, A. H. and Cohen, R. C.: The weekend effect within and downwind of Sacramento - Part 1: Observations of ozone, nitrogen oxides, and VOC reactivity, *Atmos. Chem. Phys.*, 7(20), 5327–5339, doi:10.5194/acp-7-5327-2007, 2007.
- Ngarambe, J., Nganyiyimana, J., Kim, I., Santamouris, M. and Young Yun, G.: Synergies between urban heat island and heat waves in Seoul: The role of wind speed and land use characteristics, *PLoS One*, 15(12 December), doi:10.1371/journal.pone.0243571, 2020.
- 515 Ning, G., Yim, S. H. L., Wang, S., Duan, B., Nie, C., Yang, X., Wang, J. and Shang, K.: Synergistic effects of synoptic weather patterns and topography on air quality: a case of the Sichuan Basin of China, *Clim. Dyn.*, 53(11), 6729–6744, doi:10.1007/s00382-019-04954-3, 2019.
- Ning, G., Yim, S. H. L., Yang, Y., Gu, Y. and Dong, G.: Modulations of synoptic and climatic changes on ozone pollution and its health risks in mountain-basin areas, *Atmos. Environ.*, 240, 117808, doi:10.1016/j.atmosenv.2020.117808, 2020.
- 520 Pattenden, S., Armstrong, B., Milojevic, A., Heal, M. R., Chalabi, Z., Doherty, R., Barratt, B., Kovats, R. S., Wilkinson, P., Pattenden, S., Armstrong, B., Milojevic, A., Heal, M. R., Chalabi, Z., Doherty, R., Barratt, B., Kovats, R. S. and Wilkinson, P.: Ozone, heat and mortality: acute effects in 15 British conurbations, *Occup. Environ. Med.*, 67(10), 699–707, doi:10.1136/oem.2009.051714, 2010.
- 525 Patz, J. A., Campbell-Lendrum, D., Holloway, T. and Foley, J. A.: Impact of regional climate change on human health, *Nature*, 438(7066), 310–317, doi:10.1038/nature04188, 2005.
- Pope, R. J., Butt, E. W., Chipperfield, M. P., Doherty, R. M., Fenech, S., Schmidt, A., Arnold, S. R. and Savage, N. H.: The impact of synoptic weather on UK surface ozone and implications for premature mortality, *Environ. Res. Lett.*, 11(12), doi:10.1088/1748-9326/11/12/124004, 2016.
- 530 Rastogi, D.: Revisiting Recent U . S . Heat Waves in a Warmer and More Humid Climate, *Geophys. Res. Lett.*, 47(9), 1–11, doi:10.1029/2019GL086736, 2020.
- Ren, G. Y., Chu, Z. Y., Chen, Z. H. and Ren, Y. Y.: Implications of temporal change in urban heat island intensity observed at Beijing and Wuhan stations, *Geophys. Res. Lett.*, 34(5), 1–5, doi:10.1029/2006GL027927, 2007.
- Rothfus, L.: The heat index equation, *Natl. Weather Serv. Tech. Attach.*, SR:23-90 [online] Available from: https://www.weather.gov/media/ffc/ta_htindx.PDF, 1990.
- 535 Sartor, F., Rene, S., Claude, D. and Denise, W.: Temperature, ambient ozone levels, and mortality during summer, 1994, in Belgium, *Environ. Res.*, 70, 105–113, doi:10.1006/enrs.1995.1054, 1995.
- Sillman, S.: The relation between ozone, NOx and hydrocarbons in urban and polluted rural environments, *Dev. Environ. Sci.*, 33(12), 1821–1845, doi:10.1016/S1474-8177(02)80015-8, 1999.

- 540 Tan, J., Zheng, Y., Tang, X., Guo, C., Li, L., Song, G., Zhen, X., Yuan, D., Kalkstein, A. J., Li, F. and Chen, H.: The urban heat island and its impact on heat waves and human health in Shanghai, *Int. J. Biometeorol.*, 54(1), 75–84, doi:10.1007/s00484-009-0256-x, 2010.
- Trainer, M., Williams, E., Parrish, D., Buhr, M., Allwine, E., Westberg, H., Fehsenfeld, F. and Liu, S.: Models and observations of the impact of natural hydrocarbons on rural ozone, *Nature*, 329(6164), 705–707, doi:10.1038/329705a0, 1987.
- 545 Wang, H., Wu, K., Liu, Y., Sheng, B., Lu, X., He, Y., Xie, J., Wang, H. and Fan, S.: Role of Heat Wave-Induced Biogenic VOC Enhancements in Persistent Ozone Episodes Formation in Pearl River Delta, *J. Geophys. Res. Atmos.*, 126(12), 1–19, doi:10.1029/2020JD034317, 2021a.
- Wang, J., Chen, Y., Liao, W., He, G., Tett, S. F. B., Yan, Z., Zhai, P., Feng, J., Ma, W., Huang, C. and Hu, Y.: Anthropogenic emissions and urbanization increase risk of compound hot extremes in cities, *Nat. Clim. Chang.*, doi:10.1038/s41558-021-01196-2, 2021b.
- 550 Wang, K., Wang, J., Wang, P., Sparrow, M., Yang, J. and Chen, H.: Influences of urbanization on surface characteristics as derived from the Moderate-Resolution Imaging Spectroradiometer: A case study for the Beijing metropolitan area, *J. Geophys. Res. Atmos.*, 112(22), 1–12, doi:10.1029/2006JD007997, 2007.
- 555 Wang, K., Jiang, S., Wang, J., Zhou, C., Wang, X. and Lee, X.: Comparing the diurnal and seasonal variabilities of atmospheric and surface urban heat islands based on the Beijing urban meteorological network, *J. Geophys. Res.*, 122(4), 2131–2154, doi:10.1002/2016JD025304, 2017.
- Wang, Y., Wild, O., Chen, X., Wu, Q., Gao, M., Chen, H., Qi, Y. and Wang, Z.: Health impacts of long-term ozone exposure in China over 2013–2017, *Environ. Int.*, 144, 106030, doi:10.1016/j.envint.2020.106030, 2020.
- 560 Werner, C., Fasbender, L., Romek, K. M., Yáñez-Serrano, A. M. and Kreuzwieser, J.: Heat Waves Change Plant Carbon Allocation Among Primary and Secondary Metabolism Altering CO₂ Assimilation, Respiration, and VOC Emissions, *Front. Plant Sci.*, 11(August), 1–17, doi:10.3389/fpls.2020.01242, 2020.
- Williams, S., Bi, P., Newbury, J., Robinson, G., Pisaniello, D., Saniotis, A. and Hansen, A.: Extreme heat and health: Perspectives from health service providers in rural and remote communities in South Australia, *Int. J. Environ. Res. Public Health*, 10(11), 5565–5583, doi:10.3390/ijerph10115565, 2013.
- 565 WMO: The global climate 2001–2010: A decade of climate extremes., World Meteorol. Organ., 2013.
- Wong, T. W., Tam, W. W. S., Yu, I. T. S., Lau, A. K. H., Pang, S. W. and Wong, A. H. S.: Developing a risk-based air quality health index, *Atmos. Environ.*, 76, 52–58, doi:10.1016/j.atmosenv.2012.06.071, 2013.
- World Health Organization: WHO global air quality guidelines. Particulate matter (PM_{2.5} and PM₁₀), ozone, nitrogen dioxide, sulfur dioxide and carbon monoxide., 2021.
- 570 Xing, Q., Sun, Z. Bin, Tao, Y., Zhang, X., Miao, S., Zheng, C. and Tong, S.: Impacts of urbanization on the temperature-cardiovascular mortality relationship in Beijing, China, *Environ. Res.*, 191, 110234, doi:10.1016/j.envres.2020.110234, 2020.

Xu, Z., Fitzgerald, G., Guo, Y., Jalaludin, B. and Tong, S.: Impact of heatwave on mortality under different heatwave definitions : A systematic review and meta-analysis, *Environ. Int.*, 89–90, 193–203, doi:10.1016/j.envint.2016.02.007, 2016.

575 Yang, P., Ren, G. and Liu, W.: Spatial and temporal characteristics of Beijing urban heat island intensity, *J. Appl. Meteorol. Climatol.*, 52(8), 1803–1816, doi:10.1175/JAMC-D-12-0125.1, 2013.

Yang, X., Ruby Leung, L., Zhao, N., Zhao, C., Qian, Y., Hu, K., Liu, X. and Chen, B.: Contribution of urbanization to the increase of extreme heat events in an urban agglomeration in east China, *Geophys. Res. Lett.*, 44(13), 6940–6950, doi:10.1002/2017GL074084, 2017.

580 Yang, Y., Zheng, X., Gao, Z., Wang, H., Wang, T., Li, Y., Lau, G. N. C. and Yim, S. H. L.: Long-Term Trends of Persistent Synoptic Circulation Events in Planetary Boundary Layer and Their Relationships With Haze Pollution in Winter Half Year Over Eastern China, *J. Geophys. Res. Atmos.*, 123(19), 10,991–11,007, doi:10.1029/2018JD028982, 2018.

Yang, Y., Zheng, Z., Yim, S. Y. L., Roth, M., Ren, G., Gao, Z., Wang, T., Li, Q., Shi, C., Ning, G. and Li, Y.: PM2.5
585 Pollution Modulates Wintertime Urban Heat Island Intensity in the Beijing-Tianjin-Hebei Megalopolis, China, *Geophys. Res. Lett.*, 47(1), 1–12, doi:10.1029/2019GL084288, 2020.

Yang, Y., Wang, R., Chen, F., Liu, C., Bi, X. and Huang, M.: Synoptic weather patterns modulate the frequency, type and vertical structure of summer precipitation over Eastern China: A perspective from GPM observations, *Atmos. Res.*, 249, doi:10.1016/j.atmosres.2020.105342, 2021.

590 Yim, S. H. L., Wang, M., Gu, Y., Yang, Y., Dong, G. and Li, Q.: Effect of Urbanization on Ozone and Resultant Health Effects in the Pearl River Delta Region of China, *J. Geophys. Res. Atmos.*, 124(21), 11568–11579, doi:10.1029/2019JD030562, 2019.

Yin, P., Chen, R., Wang, L., Meng, X., Liu, C., Niu, Y., Lin, Z., Liu, Y., Liu, J., Qi, J., You, J., Zhou, M. and Kan, H.: Ambient ozone pollution and daily mortality: A nationwide study in 272 Chinese cities, *Environ. Health Perspect.*, 125(11), 1–7, doi:10.1289/EHP1849, 2017.

595 Yu, S., Yin, S., Zhang, R., Wang, L., Su, F., Zhang, Y. and Yang, J.: Spatiotemporal characterization and regional contributions of O3 and NO2: An investigation of two years of monitoring data in Henan, China, *J. Environ. Sci. (China)*, 90(November), 29–40, doi:10.1016/j.jes.2019.10.012, 2020.

Zanis, P., Monks, P. S., Schuepbach, E., Carpenter, L. J., Green, T. J., Mills, G. P., Bauguitte, S. and Penkett, S. A.: In situ ozone production under free tropospheric conditions during FREETEX '98 in the Swiss Alps, *J. Geophys. Res. - Atmos.*, 105, 24223–24234, 2000.

600 Zhang, W. and Villarini, G.: On the weather types that shape the precipitation patterns across the U.S. Midwest, *Clim. Dyn.*, 53(7–8), 4217–4232, doi:10.1007/s00382-019-04783-4, 2019.

Zhang, Y., Yu, C., Bao, J. and Li, X.: Impact of temperature on mortality in Hubei, China: A multi-county time series
605 analysis, *Sci. Rep.*, 7, 45093, doi:10.1038/srep45093, 2017.

- Zhang, Z., Zhang, X., Gong, D., Quan, W., Zhao, X., Ma, Z. and Kim, S. J.: Evolution of surface O₃ and PM_{2.5} concentrations and their relationships with meteorological conditions over the last decade in Beijing, *Atmos. Environ.*, 108, 67–75, doi:10.1016/j.atmosenv.2015.02.071, 2015.
- Zhao, Z. and Wang, Y.: Influence of the West Pacific subtropical high on surface ozone daily variability in summertime over eastern China, *Atmos. Environ.*, 170, 197–204, doi:10.1016/j.atmosenv.2017.09.024, 2017.
- 610 Zheng, Z., Ren, G., Wang, H., Dou, J., Gao, Z., Duan, C., Li, Y., Ngarukiyimana, J. P., Zhao, C., Cao, C., Jiang, M. and Yang, Y.: Relationship Between Fine-Particle Pollution and the Urban Heat Island in Beijing, China: Observational Evidence, *Boundary-Layer Meteorol.*, 169(1), 93–113, doi:10.1007/s10546-018-0362-6, 2018.
- Zheng, Z., Zhao, C., Lolli, S., Wang, X., Wang, Y., Ma, X., Li, Q. and Yang, Y.: Diurnal variation of summer precipitation modulated by air pollution: Observational evidences in the beijing metropolitan area, *Environ. Res. Lett.*, 15(9), 615 doi:10.1088/1748-9326/ab99fc, 2020.
- Zong, L., Yang, Y., Gao, M., Wang, H., Wang, P., Zhang, H., Wang, L., Ning, G., Liu, C., Li, Y. and Gao, Z.: Large-scale synoptic drivers of co-occurring summertime ozone and PM_{2.5} pollution in eastern China, *Atmos. Chem. Phys.*, 21, 9105–9124, doi:10.5194/acp-21-9105-2021, 2021a.
- 620 Zong, L., Liu, S., Yang, Y., Ren, G., Yu, M., Zhang, Y. and Li, Y.: Synergistic Influence of Local Climate Zones and Wind Speeds on the Urban Heat Island and Heat Waves in the Megacity of Beijing, China, *Front. Earth Sci.*, 9, 458, doi:10.3389/feart.2021.673786, 2021b.

625

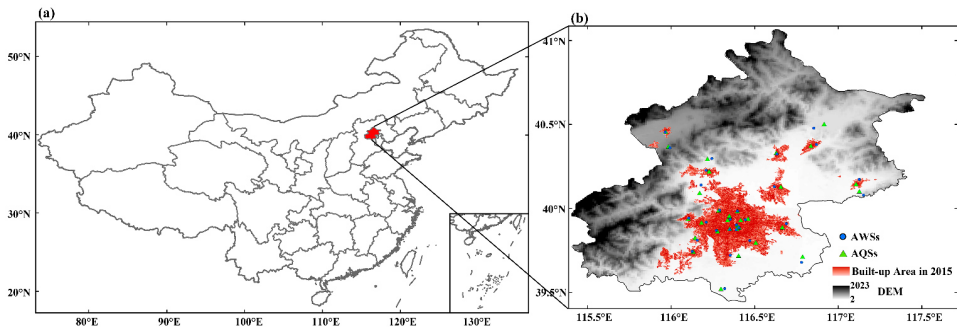


Figure 1: (a) Geography of Beijing. (b) Distribution of AWSs and air quality stations (AQSS) in Beijing (superimposed on the built-up area data for 2015 from digital elevation model data).

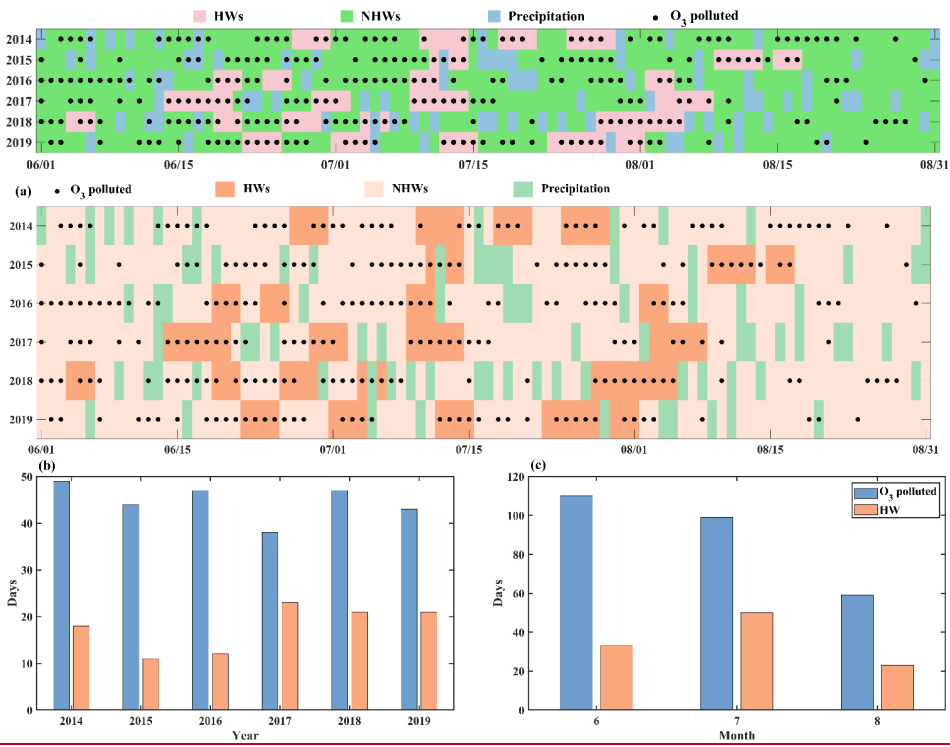
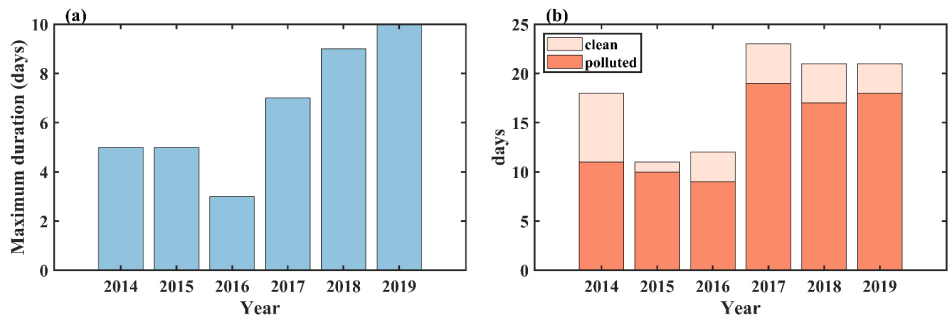


Figure 2: (a) Time series of weather types, in which the black dots indicate O₃ pollution that occurred on that day. Interannual (b) and intermonthly (c) variations in O₃ pollution and HW days.

630



635 Figure 3: (a) Maximum number of days of HW events each year. (b) Proportion of O₃ pollution during HW events each year.

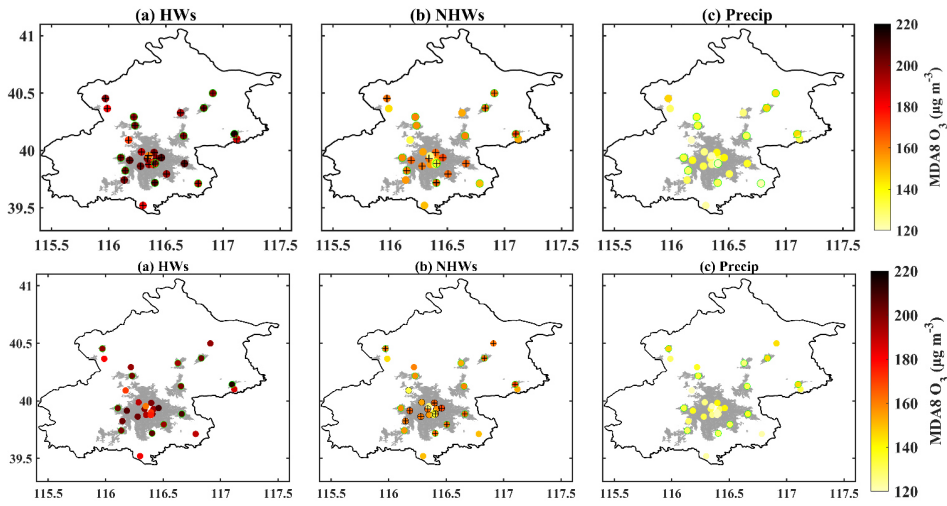
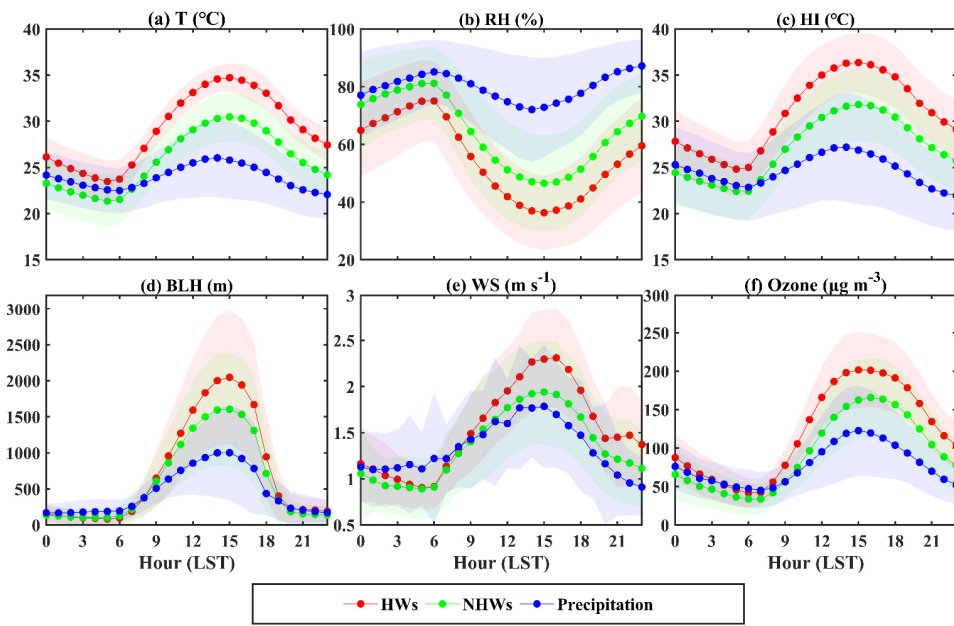


Figure 4: Distribution of MDA8 O₃ under (a) HWs, (b) NHWs, and (c) precipitation periods (superimposed on built-up area data for 2015, with green dots indicating vegetation covered stations, black and green circles represent urban and suburban stations, respectively). The diurnal variation of (d) air temperature, (e) RH, (f) HI, (g) BLH, (h) WS and (i) O₃, under HWs, NHWs and precipitation periods (shading indicates standard deviation).

640

645



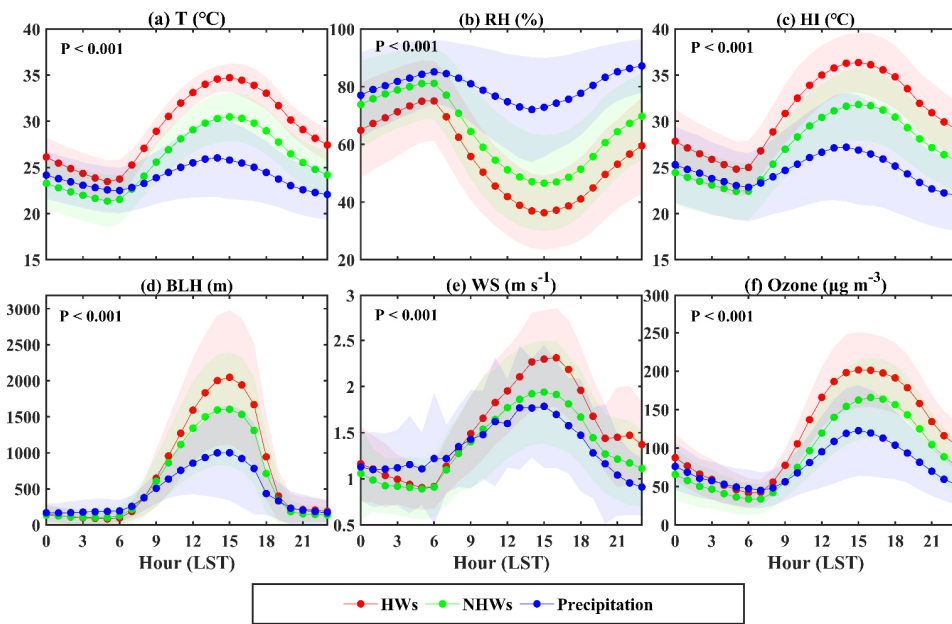


Figure 5: The diurnal variation of (a) air temperature, (b) RH, (c) HI, (d) BLH, (e) WS and (f) O₃, under HWs, NHWs and precipitation periods (shading indicates standard deviation, **P < 0.001 means pass the significance test**).

650

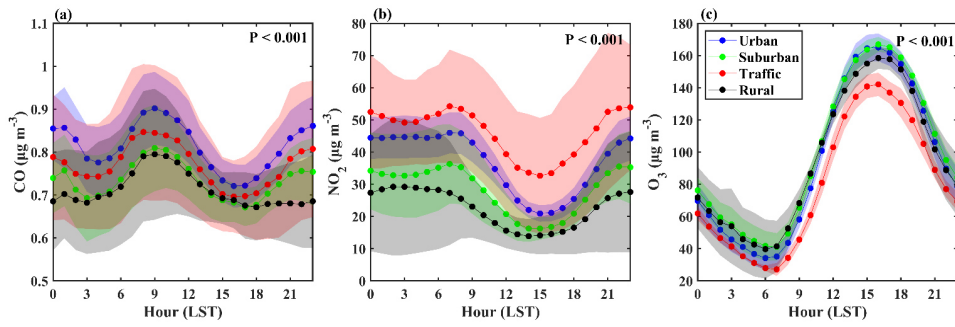
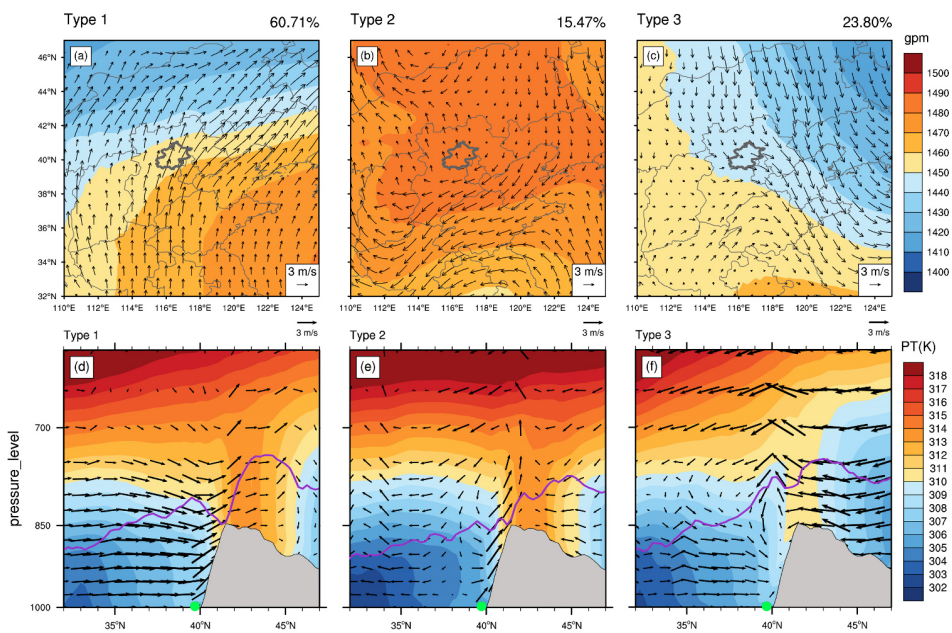
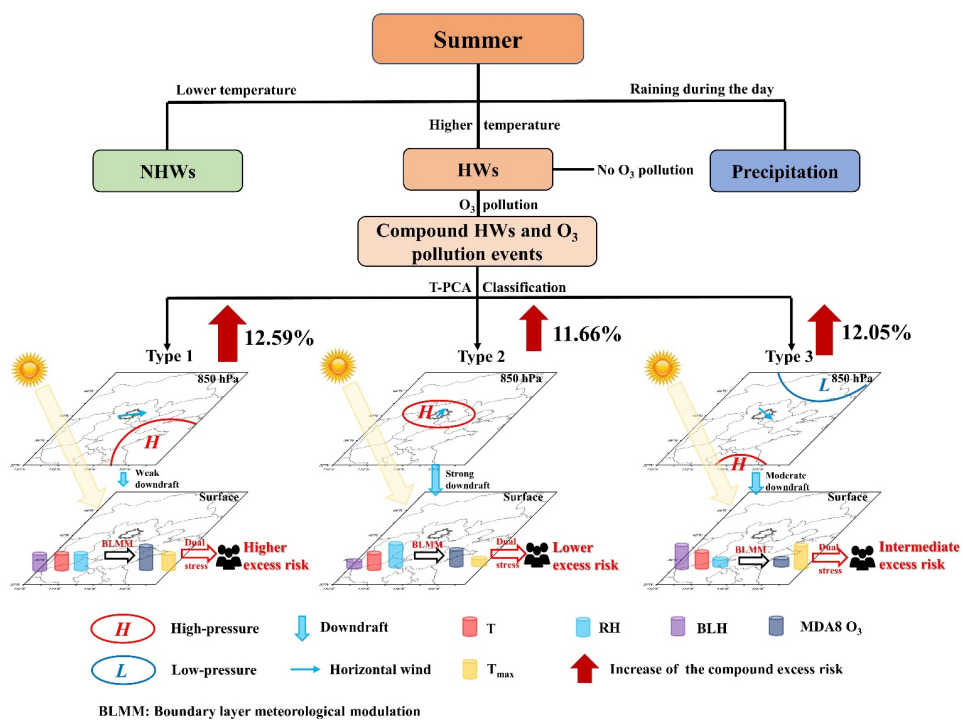


Figure 6: The diurnal variation of (a) CO, (b) NO₂, (c) O₃, under different stations (shading indicates standard deviation, P < 0.001 means pass the significance test).



660 | **Figure 67:** (a–c) 850-hPa GH (contours) and vv-wind (vectors) patterns related to HWs and O₃ pollution compound events based on objective classification (grey outline represents Beijing, and the number in the upper-right corner of each panel indicates the frequency of occurrence of each pattern). (d–f) Vertical cross-sections of the potential temperature (contours) and wind vectors (synthesized by v and scaled ω, ω scaled by 100) averaged between 116.0°E and 117.0°E associated with the synoptic patterns (purple solid lines mark the BLH, black contours mark the topography, and the green dot marks the location of Beijing).



665 | Figure 78: Schematic illustration of the mechanism of HW and O₃ compound pollution events under different synoptic weather patterns (height of the icon indicates the size of each variable).

Table 1: The location information and station type of AQSs, the corresponding AWSs are the closest matching weather station among 295 AWSs.

AQI StationSs	Lon (°)	Lat (°)	Type	AWS	Lon (°)	Lat (°)
DS	116.42	39.93	Urban	A1003	116.44	39.93
TT	116.41	39.89	Urban*	A1016	116.41	39.88
GY	116.34	39.93	Urban	A1006	116.35	39.93
WSXG	116.35	39.88	Urban	A1015	116.35	39.87
ATZX	116.40	39.98	Urban	A1007	116.40	39.98
NZG	116.46	39.94	Urban	A1003	116.44	39.93
WL	116.29	39.99	Urban	54399	116.29	39.99
BBXQ	116.17	40.09	Urban	A1033	116.18	40.14
FTHY	116.28	39.86	Urban	A1053	116.27	39.87
YG	116.15	39.82	Urban*	A1037	116.16	39.81
GC	116.18	39.91	Urban	A1019	116.21	39.92
FS	116.14	39.74	Rural Suburban	A1314	116.13	39.74
DX	116.40	39.72	Suburban Rural*	54594	116.35	39.72
YZ	116.51	39.80	Suburban Rural	54511	116.47	39.81
TZ	116.66	39.89	Suburban Rural	A1213	116.69	39.91
SY	116.66	40.13	Suburban Rural*	54398	116.62	40.13
CP	116.23	40.22	Suburban Rural*	54499	116.21	40.22
MTG	116.11	39.94	Suburban Rural*	A1354	116.11	39.94
PG	117.10	40.14	Suburban Rural*	54424	117.12	40.17
HR	116.63	40.33	Suburban Rural	A1621	116.63	40.32
MY	116.83	40.37	Suburban Rural*	54416	116.86	40.38
YQ	115.97	40.45	Suburban Rural	54406	115.97	40.45
QM	116.40	39.90	Traffic	A1001	116.39	39.90
YDM	116.39	39.88	Traffic	A1020	116.39	39.87
XZMB	116.35	39.95	Traffic	A1006	116.35	39.93
DL	116.22	40.29	Other Rural*	A1407	116.25	40.29
BDL	115.99	40.37	Rural Other	A1468	116.00	40.36
MYSK	116.91	40.50	Rural Other*	A1655	116.85	40.47

DGC	117.12	40.10	RuralOther*	A1514	117.14	40.08
YLD	116.78	39.71	RuralOther	A1201	116.78	39.68
YF	116.30	39.52	RuralOther	A1252	116.32	39.52

Note: The asterisk in the type column indicates that the underlying surface of the observing station is covered by vegetation.

670

Table 2: Analysis of variance of each variable under different weather conditions (HWs, NHWs and precipitation).

	Source	SS	df	MS	F	P
T_{max}	Group	2609.52	2	1304.76	215.27	1.09E-69
	Error	3315.38	547	6.06		
	Total	5924.89	549			
	Source	SS	df	MS	F	P
MDA8O₃	Group	204454.6	2	102227.3	56.32	6.03E-23
	Error	981941.2	541	1815		
	Total	1186396	543			
	Source	SS	df	MS	F	P
ER_{UV}	Group	2614.65	2	1307.33	221.48	3.46E-71
	Error	3228.8	547	5.9		
	Total	5843.45	549			
	Source	SS	df	MS	F	P
ER_{ozone}	Group	353.62	2	176.808	56.4	5.63E-23
	Error	1695.85	541	3.135		
	Total	2049.47	543			
	Source	SS	df	MS	F	P
ER_{total}	Group	4867.9	2	2433.94	207.28	1.69E-67
	Error	6329.2	539	11.74		
	Total	11197.1	541			

675 Table 32: RH, temperature, HI, MDA8 O₃, O₃ concentration, and ER of HW and O₃ pollution compound events for mortalities in different station types associated with different weather conditions.

Station type	Period	RH (%)	T _{mean} (°C)	T _{min} (°C)	T _{max} (°C)	HI _{min} (°C)	HI _{mean} (°C)	HI _{max} (°C)	MDA8 O ₃ (µg·m ⁻³)	O ₃ mean (µg·m ⁻³)	ER _{HW} (%)	ER _{MDA8} (%)	ER _{total} (%)
Urban	HWs	53.8	30.1	24.0	36.1	32.0	25.3	38.3	197.1	119.8	4.76(4.76;4.77)	8.01(0.79;16.00)	12.78(5.56;20.78)
	NHWs	62.4	26.6	21.6	31.8	27.8	22.0	33.3	158.5	91.5	0.3179(0.3175;0.3186)	6.40(0.64;12.70)	6.69(0.94;12.99)
	Precip	80.1	24.4	21.4	28.5	25.1	19.8	31.0	130.6	73.5	-2.868(-2.87; -2.866)	5.24(0.52;10.36)	2.38(-2.34;7.49)
Rural	HWs	56.7	29.0	23.0	34.8	30.8	24.0	36.8	201.8	126.5	3.403(3.400;3.410)	8.21(0.81;16.42)	11.61(4.22;19.83)
	NHWs	64.5	25.7	20.7	30.7	26.9	21.3	32.0	161.0	96.6	-0.798(-0.799;-0.797)	6.50(0.65;12.92)	5.67(-0.17;12.08)
	Precip	79.1	23.9	20.8	27.8	24.7	19.7	30.0	135.7	79.4	-3.553(-3.550;-3.561)	5.45(0.54;10.79)	1.88(-3.02;7.21)
Traffic	HWs	50.3	30.4	25.2	35.8	32.1	26.7	37.6	169.7	118.9	4.412(4.408;4.421)	6.86(0.68;13.63)	11.28(5.09;18.06)
	NHWs	59.0	26.9	22.4	31.6	28.2	23.3	32.9	132.8	93.8	0.1092(0.1090;0.1095)	5.33(0.53;10.53)	5.42(0.63;10.61)
	Precip	77.3	24.5	21.6	28.5	25.3	20.3	30.6	106.2	78.7	-2.947(-2.944;-2.952)	4.24(0.43;8.35)	1.28(-2.54;5.38)
All	HWs	55.5	29.4	23.5	35.2	31.2	24.6	37.4	189.4	117.4	3.867(3.863;3.875)	7.90(0.78;15.78)	11.78(4.66;19.66)
	NHWs	63.8	25.9	21.1	31.0	27.2	21.6	32.6	151.4	89.6	-0.4179(-0.4175;-0.4183)	6.29(0.63;12.49)	5.85(0.2;12.03)
	Precip	79.7	24.0	20.9	28.0	24.7	19.7	30.4	125.9	72.5	-3.377(-3.374;-3.384)	5.23(0.52;10.33)	1.84(-2.86;6.94)
Ur-Ru	HWs	-2.9	1.0	1.1	1.3	1.2	1.3	1.5	-4.7	-6.2	1.36	-0.20	1.17
	NHWs	-2.3	0.9	0.9	1.1	0.9	0.7	1.3	-2.5	-5.1	1.12	-0.10	1.02
	Precip	0.9	0.5	0.5	0.7	0.4	0.1	1.0	-5.1	-5.9	0.08	-0.21	0.50
Urban	HWs	53.8	30.1	24.0	36.1	32.0	25.3	38.3	197.1	119.8	4.76(4.76;4.77)	8.01(0.79;16.00)	12.78(5.56;20.78)
	NHWs	62.4	26.6	21.6	31.8	27.8	22.0	33.3	158.5	91.5	0.3179(0.3175;0.3186)	6.40(0.64;12.70)	6.69(0.94;12.99)
	Precip	80.1	24.4	21.4	28.5	25.1	19.8	31.0	130.6	73.5	-2.868(-2.87; -2.866)	5.24(0.52;10.36)	2.38(-2.34;7.49)
Suburban	HWs	56.7	29.0	23.0	34.8	30.8	24.0	36.8	201.8	126.5	3.403(3.400;3.410)	8.21(0.81;16.42)	11.61(4.22;19.83)
	NHWs	64.5	25.7	20.7	30.7	26.9	21.3	32.0	161.0	96.6	-0.798(-0.799;-0.797)	6.50(0.65;12.92)	5.67(-0.17;12.08)
	Precip	79.1	23.9	20.8	27.8	24.7	19.7	30.0	135.7	79.4	-3.553(-3.561;-3.550)	5.45(0.54;10.79)	1.88(-3.02;7.21)
Traffic	HWs	50.3	30.4	25.2	35.8	32.1	26.7	37.6	169.7	118.9	4.412(4.408;4.421)	6.86(0.68;13.63)	11.28(5.09;18.06)
	NHWs	59.0	26.9	22.4	31.6	28.2	23.3	32.9	132.8	93.8	0.1092(0.1090;0.1095)	5.33(0.53;10.53)	5.42(0.63;10.61)
	Precip	77.3	24.5	21.6	28.5	25.3	20.3	30.6	106.2	78.7	-2.947(-2.952;-2.944)	4.24(0.43;8.35)	1.28(-2.54;5.38)
Rural	HWs	61.0	27.9	21.7	34.2	29.9	22.4	36.9	188.7	119.5	2.786(2.785;2.793)	7.66(0.75;15.29)	10.45(3.55;18.09)
	NHWs	69.3	24.6	19.5	30.1	25.9	19.9	32.1	153.2	93.6	-1.344(-1.347;-1.343)	6.18(0.61;12.26)	4.78(-0.76;10.85)
	Precip	82.1	23.1	20.0	27.1	23.9	19.0	29.9	131.1	79.2	-4.207(-4.215;-4.203)	5.26(0.53;10.41)	1.03(-3.70;6.617)
All	HWs	55.5	29.4	23.5	35.2	31.2	24.6	37.4	189.4	117.4	3.867(3.863;3.875)	7.90(0.78;15.78)	11.78(4.66;19.66)
	NHWs	63.8	25.9	21.1	31.0	27.2	21.6	32.6	151.4	89.6	-0.4179(-0.4187;-0.4175)	6.29(0.63;12.49)	5.85(0.2;12.03)
	Precip	79.7	24.0	20.9	28.0	24.7	19.7	30.4	125.9	72.5	-3.377(-3.384;-3.374)	5.23(0.52;10.33)	1.84(-2.86;6.94)
Ur-Ru	HWs	-7.2	2.2	2.3	1.9	2.1	2.9	1.4	8.4	0.3	1.97	0.35	2.33
	NHWs	-6.9	2	2.1	1.7	1.9	2.1	1.2	5.3	-2.1	1.67	0.22	1.91
	Precip	-2	1.3	1.4	1.4	1.2	0.8	1.1	-0.5	-5.7	1.3	-0.02	1.35

Note: Ur-Ru: Urban-Rural. Red color indicates groups with greater ER.

680 **Table 43:** RH, temperature, HI, MDA8 O₃, O₃ concentration, and ER of HW and O₃ compound pollution events for mortalities at different station types associated with different synoptic patterns.

Station type	Period	RH (%)	T _{max} (°C)	T _{min} (°C)	T _{avg} (°C)	HI _{max} (°C)	HI _{min} (°C)	HI _{avg} (°C)	MDA8 O ₃ (µg·m ⁻³)	O ₃ mean (µg·m ⁻³)	ER _{HW} (%)	ER _{O₃} (%)	ER _{compound} (%)
Urban	Type-1	55.9	30.3	24.6	36.0	32.8	26.0	39.2	216.3	133.1	4.65(4.64,4.66)	8.81(0.87,17.66)	13.45(5.50,22.30)
	Type-2	64.0	30.5	25.5	35.7	34.5	27.7	40.8	206.2	121.6	4.40(4.39,4.41)	8.38(0.83,16.76)	12.78(5.22,21.16)
	Type-3	49.7	29.5	22.6	36.4	29.9	23.2	36.4	201.4	122.4	5.06(5.05,5.07)	8.18(0.81,16.34)	13.24(5.86,21.41)
Rural	Type-1	58.2	29.4	23.6	34.8	31.6	24.8	37.7	225.6	142.6	3.381(3.378,3.388)	9.21(0.91,18.49)	12.59(4.28,21.88)
	Type-2	66.7	29.5	24.2	34.7	33.0	25.4	39.4	202.8	123.3	3.278(3.275,3.285)	8.24(0.81,16.46)	11.53(4.09,19.77)
	Type-3	53.0	28.4	21.5	35.0	28.9	22.0	35.0	201.3	127.4	3.538(3.534,3.545)	8.18(0.81,16.35)	11.71(4.33,19.89)
Traffic	Type-1	52.2	30.8	25.8	35.7	32.9	27.5	38.4	185.9	116.3	4.341(4.337,4.350)	7.53(0.75,15.02)	11.87(5.08,19.35)
	Type-2	59.7	30.8	26.5	35.6	34.4	29.3	39.5	175.8	101.2	4.161(4.157,4.170)	7.11(0.71,14.13)	11.24(4.83,18.27)
	Type-3	46.6	29.7	23.5	35.8	30.1	24.6	35.7	174.8	108.6	4.462(4.457,4.471)	7.06(0.70,14.03)	11.52(5.16,18.5)
All	Type-1	57.2	29.7	24.1	35.2	32.0	25.4	38.3	209.3	131.3	3.796(3.792,3.804)	8.80(0.87,17.63)	12.59(4.66,21.42)
	Type-2	65.5	29.8	24.7	35.0	33.5	26.5	39.9	195.0	114.5	3.644(3.640,3.651)	8.00(0.79,15.97)	11.66(4.44,19.64)
	Type-3	51.6	28.7	22.0	35.4	29.2	22.5	35.5	192.5	120.0	4.063(4.059,4.071)	7.99(0.79,15.95)	12.05(4.85,20.02)
Ur-Ru	Type-1	-2.37	1.0	1.0	1.2	1.1	1.1	1.5	-9.3	-9.5	1.27	-0.40	0.86
	Type-2	-2.74	1.0	1.3	1.0	1.4	2.3	1.4	3.4	-1.7	1.12	0.16	1.25
	Type-3	-3.33	1.1	1.1	1.4	1.1	1.3	1.4	0.1	-5.0	1.52	0	1.53
Station type	Period	RH (%)	T _{max} (°C)	T _{min} (°C)	T _{avg} (°C)	HI _{max} (°C)	HI _{min} (°C)	HI _{avg} (°C)	MDA8 O ₃ (µg·m ⁻³)	O ₃ mean (µg·m ⁻³)	ER _{HW} (%)	ER _{O₃} (%)	ER _{compound} (%)
Urban	Type 1	55.9	30.3	24.6	36.0	32.8	26.0	39.2	216.3	133.1	4.65(4.64,4.66)	8.81(0.87,17.66)	13.45(5.50,22.30)
	Type 2	64.0	30.5	25.5	35.7	34.5	27.7	40.8	206.2	121.6	4.40(4.39,4.41)	8.38(0.83,16.76)	12.78(5.22,21.16)
	Type 3	49.7	29.5	22.6	36.4	29.9	23.2	36.4	201.4	122.4	5.06(5.05,5.07)	8.18(0.81,16.34)	13.24(5.86,21.41)
Suburban	Type 1	58.2	29.4	23.6	34.8	31.6	24.8	37.7	225.6	142.6	3.381(3.378,3.388)	9.21(0.91,18.49)	12.59(4.28,21.88)
	Type 2	66.7	29.5	24.2	34.7	33.0	25.4	39.4	202.8	123.3	3.278(3.275,3.285)	8.24(0.81,16.46)	11.53(4.09,19.77)
	Type 3	53.0	28.4	21.5	35.0	28.9	22.0	35.0	201.3	127.4	3.538(3.534,3.545)	8.18(0.81,16.35)	11.71(4.33,19.89)
Traffic	Type 1	52.2	30.8	25.8	35.7	32.9	27.5	38.4	185.9	116.3	4.341(4.337,4.350)	7.53(0.75,15.02)	11.87(5.08,19.35)
	Type 2	59.7	30.8	26.5	35.6	34.4	29.3	39.5	175.8	101.2	4.161(4.157,4.170)	7.11(0.71,14.13)	11.24(4.83,18.27)
	Type 3	46.6	29.7	23.5	35.8	30.1	24.6	35.7	174.8	108.6	4.462(4.457,4.471)	7.06(0.70,14.03)	11.52(5.16,18.5)
Rural	Type 1	62.6	27.7	21.6	34.0	29.8	22.2	37.0	195.4	120.4	2.718(2.715,2.724)	8.63(0.85,17.30)	11.33(3.55,20.00)
	Type 2	73.6	27.8	22.8	33.1	31.2	22.6	38.9	168.3	103.3	2.671(2.669,2.677)	7.25(0.72,14.40)	9.95(3.42,17.14)
	Type 3	60.8	26.2	19.9	33.1	27.4	20.5	34.1	171.8	105.4	2.972(2.969,2.978)	7.75(0.77,15.46)	10.70(3.73,18.41)
All	Type 1	57.2	29.7	24.1	35.2	32.0	25.4	38.3	209.3	131.3	3.796(3.792,3.804)	8.80(0.87,17.63)	12.59(4.66,21.42)
	Type 2	65.5	29.8	24.7	35.0	33.5	26.5	39.9	195.0	114.5	3.644(3.640,3.651)	8.00(0.79,15.97)	11.66(4.44,19.64)
	Type 3	51.6	28.7	22.0	35.4	29.2	22.5	35.5	192.5	120.0	4.063(4.059,4.071)	7.99(0.79,15.95)	12.05(4.85,20.02)
Ur-Ru	Type 1	-6.7	2.6	3	2	3	3.8	2.2	20.9	12.7	1.93	0.18	2.12
	Type 2	-9.6	2.7	2.7	2.6	3.3	5.1	1.9	37.9	18.3	1.73	1.13	2.83
	Type 3	-11.1	3.3	2.7	3.3	2.5	2.7	2.3	29.6	17	2.03	0.33	2.54

Note: Ur-Ru: Urban-Rural. Red color indicates groups with greater ER.

685 Table 54: Contribution rate of urbanization and weather type to ER.

Source	CR		
	ER _{HW}	ER _{ozone}	ER _{total}
urbanization	27.7245.68%	-2.585.05%	8.0818.95%
Type 1	85.3683.21%	25.8820.82%	46.3946.81%
Type 2	84.5182.52%	22.0712.45%	43.5836.48%
Type 3	86.5484.32%	20.1411.41%	45.5435.21%